Thermochimica Acta, 104 (1986) 159–178
Elsevier Science Publishers B.V., Amsterdam – Printed in The Netherlands

THERMAL DECOMPOSITION AND DEHYDRATION OF MAGNESIUM PERCHLORATE HEXAHYDRATE

DAVID J. DEVLIN and PATRICK J. HERLEY

Department of Materials Science and Engineering, State University of New York at Stony Brook, Stony Brook, NY 11794 (U.S.A.)

(Received 3 January 1986)

ABSTRACT

The dehydration and thermal decomposition kinetics of magnesium perchlorate hexahydrate have been studied using thermogravimetric analysis, differential scanning calorimetry and x-ray diffraction techniques in conjunction with isothermal gas evolution vs. time measurements. For $Mg(ClO_4)_2 \cdot 6H_2O$ dehydration occurs in a complex manner in three distinct temperature regions between 148–197, 248–278 and 344–395°C. Each region is associated with the removal of $2H_2O$. For $Mg(ClO_4)_2$ between 369 and 429°C the fractional decomposition, α, vs. time curves are sigmoidal and consist of an induction period, an acceleratory period followed by a short decay stage up to $\alpha \sim 0.5$ and a slow decay stage from $\alpha \sim 0.5$ to completion. Above 417°C this long decay stage is replaced by an acceleratory stage. Activation energies for the induction, acceleratory, first and second decay stages are 78.6 ± 2.0, 65.3 ± 5.6, 48.9 ± 6.4 and 58.0 ± 11.1 kcal mol^{-1}, respectively. The results suggest that decomposition proceeds via the formation of an intermediate, $(MgO \cdot MgClO_4)$, which dissociates at low temperatures and decomposes rapidly to MgO above 417°C.

The principal effects of exposure to ^{60}Co gamma rays prior to thermal decomposition is to reduce the induction period and increase the rate of the acceleratory period. These results have been interpreted as the introduction of additional nucleation sites by the irradiation and are consistent with previously reported data on irradiation effects on thermally decomposed inorganic solids.

INTRODUCTION

This report focuses on studies directed to obtain data on the dehydration and thermal decomposition kinetics of $Mg(ClO_4)_2 \cdot 6H_2O$ and includes studies on the effects of ionizing radiation on the thermal decomposition kinetics. Previously it has been shown that exposure to gamma irradiation prior to decomposition accelerates the isothermal decomposition of several solids [1] including perchlorates such as ammonium perchlorate [2] and shortens the length of the induction period, where present, in the isothermal fractional decomposition, α, vs. time curves [3]. It would be of interest to investigate whether similar effects could be induced in $Mg(ClO_4)_2 \cdot 6H_2O$.

In magnesium perchlorate the previously reported work [4–10] on the

0040-6031/86/$03.50

dehydration process is fragmented and ambiguous. Smith and Willard [4] reported that the hexahydrate melted between 145 and 147°C. Subsequent dehydration at 25°C in vacuum for four months resulted in a sample weight loss corresponding to $3H_2O$, i.e. a trihydrate salt formed. A further study [5] predicted that the di- and tetrahydrates should also exist. Later experimental work by Copeland and Bragg [6] confirmed this. However they found no evidence for the existence of a trihydrate suggesting that the earlier workers had obtained mixed crystals of the di- and tetrahydrates. Reported weight loss measurements also yield contradictory results: Marvin and Woolaver [7] reported a continuous weight loss from 30–450°C with melting whereas Acheson and Jacobs [8] found that the hexahydrate salt could be decomposed in vacuo below 230°C to yield an anhydrous powder which was stable between 23–320°C. The latter did not observe any melting of their samples. Melting with bubbling was reported by Gordon and Campbell [9] and by Zinov'ev et al. [10] in their differential thermal analysis (DTA) studies.

The isothermal decomposition of $Mg(ClO_4)_2 \cdot 6H_2O$ has been the subject of several investigations [8,11]. Solymosi [11] carried out the decomposition between 386 and 408°C in vacuum and reported that 35% of the reaction proceeded according to the equation

$$Mg(ClO_4)_2 \rightarrow MgO + Cl_2 + 3.5O_2 \quad (1)$$

The remainder decomposed according to the equation

$$Mg(ClO_4)_2 \rightarrow MgCl_2 + 4O_2. \quad (2)$$

Irregular α vs. t curves were obtained particularly above $\alpha \sim 0.5$. First order and contracting cube equations were fitted over the range $\alpha = 0.1$ to 0.7. The reported activation energy was between 40.1 and 41.2 kcal mol^{-1} for the entire reaction.

In a more detailed study Acheson and Jacobs [8] examined the isothermal decomposition kinetics between 336°C and 438°C in vacuum and under 740 Torr of nitrogen. In vacuum, the α, t curves were essentially similar to those of Solymosi [9]. The acceleratory period ($0 < \alpha < 0.1$) was fitted to a power law ($\alpha = kt^3 + c$) and the decay stage to a contracting volume equation [12]. Activation energies were not reported nor were extensive measurements carried out in vacuum. Using nitrogen gas to suppress sublimation, the acceleratory period fit remained unaltered but the decay stage fitted a contracting cube equation. Activation energies of 58.1 and 66.7 kcal mol^{-1} respectively were found for the acceleratory and decay stages. The prolonged decay stage ($0.48 < \alpha < 0.75$) was described approximately by a contracting cube equation. The rate constants of this stage were reported to be independent of temperature.

In a later study using gas chromatography Borisova et al. [13,14] reported oxygen peaks at 389, 480 and 562°C. The first peak was attributed to dehydration and partial hydrolysis of $Mg(ClO_4)_2$ with the subsequent de-

composition of $HClO_4$. The subsequent peaks were associated with a two stage decomposition of $Mg(ClO_4)_2$ to MgO involving an intermediate phase. The reaction was reported to exhibit zero order kinetics with apparent activation energies for the two decomposition stages of 83 ± 2.4 and 52 ± 3.3 kcal mol^{-1}, respectively.

EXPERIMENTAL

Materials

Crystals of magnesium perchlorate hexahydrate were prepared by recrystallization from aqueous solution. Triple distilled water was used throughout. For $Mg(ClO_4)_2 \cdot 6H_2O$ the starting materials were obtained from Allied Chemicals (percentage purity 97%) and from Alfa Products (percentage purity 98%).

For the differential scanning calorimetry (DSC) studies the needle-like crystals (5–6 cm in length) were stored in saturated aqueous solution and removed just prior to use. Small sections (10–20) mg were dried on absorbent paper and were either used directly or powdered in an agate pestle and mortar and sieved to pass through a 180 μm mesh brass sieve and be retained on a 125 μm mesh sieve.

For thermogravimetric analysis (TGA) the materials were powdered before use having been removed from their saturated solutions and stored in a desiccator over anhydrous calcium sulfate. For isothermal studies 15–20 mg of the powdered samples were decomposed in a platinum boat. The magnesium perchlorate samples were pumped continuously for 2 h in vacuum at room temperature prior to insertion in the furnace.

Equipment and procedure

DSC measurements were made in a Perkin-Elmer DSC-2 calorimeter under a flow of dry nitrogen. The spectra were run at 5–40° min^{-1} on 10–20 mg samples over the temperature range 100–600°C. When the run was interrupted the sample was cooled immediately unless otherwise noted. TGA runs were carried out on a Perkin-Elmer TGS-1 unit using a Cahn RG electrobalance under a dry nitrogen gas flow. Runs were made from 100–600°C at 10–20°C min^{-1} on 8–10 mg samples.

Isothermal decomposition measurements were made in a conventional Pyrex-glass constant-volume high vacuum system using a specifically constructed decomposition chamber [2]. The pressure in the system was measured with a fused-quartz Bourdon-tube pressure gauge, Texas Instruments model 145, digitized via a shaft encoder to read the pressure in times varying from 3 s upwards. Prior to decomposition the background pressure in the

system with all traps and pumps operating was less than 1×10^{-4} Pa. During a typical run a liquid nitrogen trap was present always between the decomposition chamber and the manometer.

X-ray diffraction measurements were made on a Debye Scherrer camera using radiation from a Fe target (Mn filter) from a General Electric XRD5 unit at 35 kV and 15 ma. Samples were sealed in 0.5 mm diameter glass capillary tubes.

Irradiations were carried out with 1.1 and 1.3 MeV ^{60}Co gamma rays at the spent fuel facility at Brookhaven National Laboratory. The samples were sealed under dry nitrogen in pre-baked fused silica ampoules and irradiated in the dark at ambient temperature. The gamma-ray dose rates used were 1.3 and 3.6×10^6 rad h^{-1}.

RESULTS

Isothermal decomposition

The fractional decomposition, α, vs. time plots for the isothermal decomposition are sigmoid shaped (Fig. 1). At the lowest temperature studied (369°C) the curves consist of a short, linear induction period followed by an acceleratory period which transfers to a decay period at $\alpha \sim 0.2$. The curves for the decay period appear to consist of a short, sharp deceleratory period

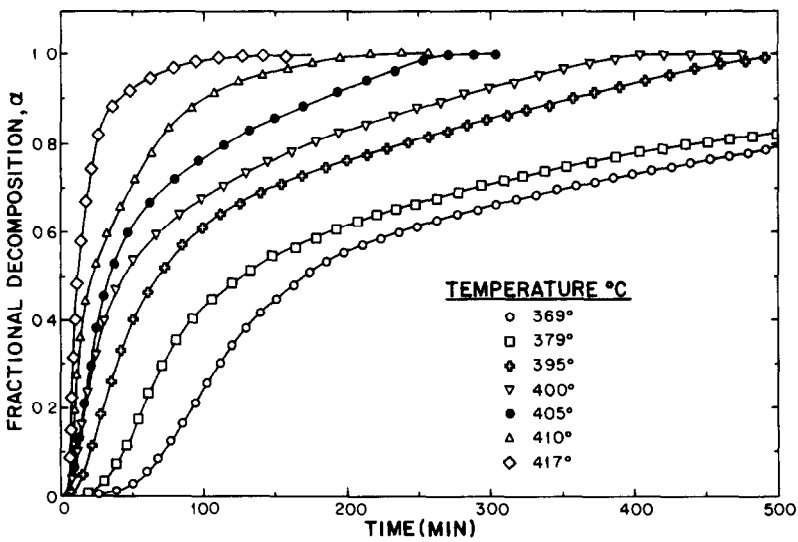

Fig. 1. Effect of temperature on the isothermal decomposition of magnesium perchlorate powder in vacuo. The plot shows the fractional decomposition, $\alpha = p(t)/p_f$, vs. time curves for gas evolution from 25 mg of magnesium perchlorate powder between 369 and 417°C.

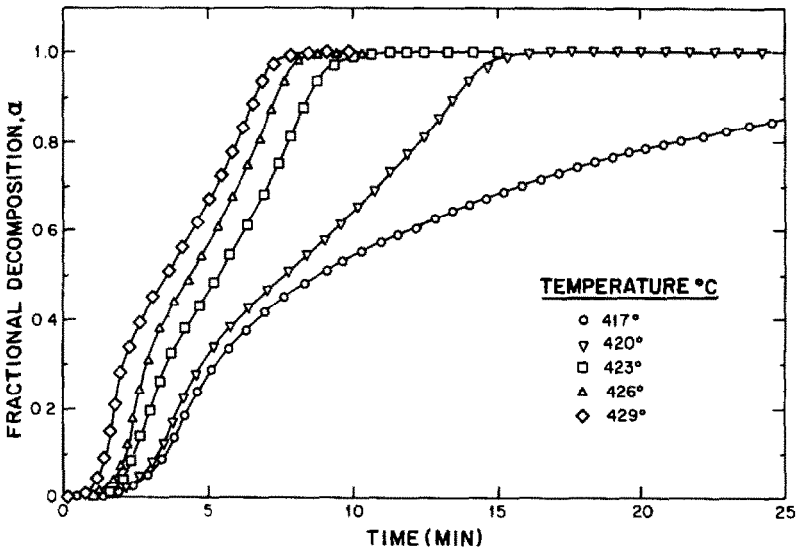

Fig. 2. Effect of temperature on the isothermal decomposition of magnesium perchlorate powder in vacuo. The plot shows the fractional decomposition, $\alpha = p(t)/p_f$ vs. time curves for gas evolution from 25 mg of magnesium perchlorate powder between 417 and 429°C. This figure complements Fig. 1.

merging into a long, slowly decreasing curve which extends to the completion of the reaction and comprises essentially half of the entire fractional decomposition. Together the two decay stages comprise 80% of the entire decomposition.

Above 417°C another interesting effect occurs. The α, t curves change shape and a second acceleratory period develops during the sharp decay stages (Fig. 2) at approximately $\alpha = 0.4$. The α, t curves terminate abruptly following this period. This second acceleratory stage persists to the highest temperature studied (429°C). This is indicative of the onset of a second decomposition process initiating at ~ 420°C during the decay stage of the first process and comprising ~ 50% of the fractional decomposition. The final pressure normalized to a constant weight of solid remains constant over the entire decomposition temperature range (417–369°C).

The total gas pressure vs. time curves over the induction, acceleratory and sharp decay periods are satisfactorily reproducible (Fig. 3). However the extent of the final slow decay period was difficult to characterize particularly at low temperatures due to the slow merger of the evolved gas rate into the background outgassing rate of the apparatus.

A series of experiments was carried out to elucidate some of the physical processes occurring during the decomposition:

(a) When the α, t data of dehydrated, thermally decomposed material is compared with data from the thermal decomposition of hexahydrate at

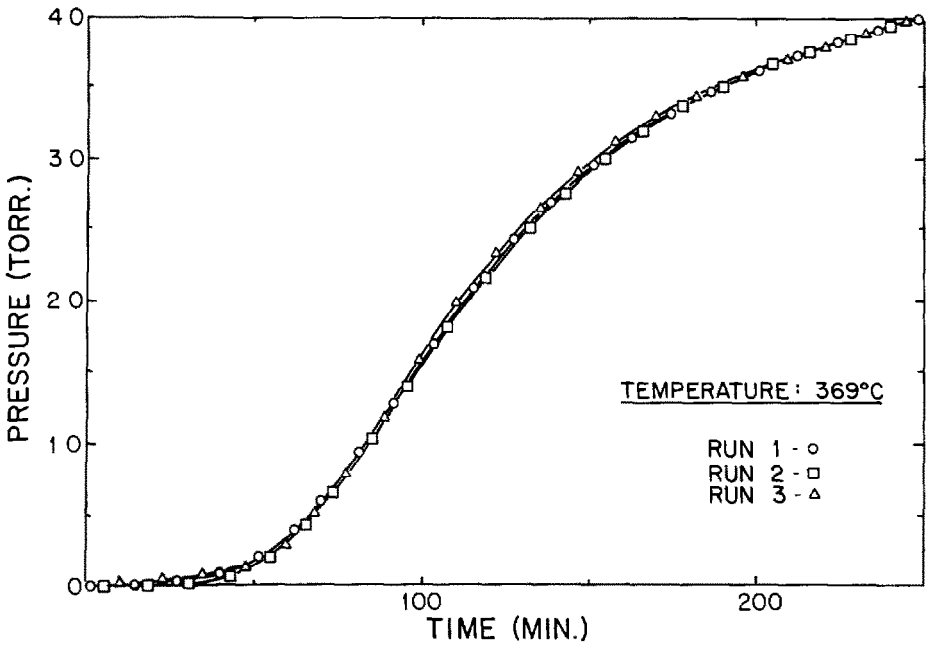

Fig. 3. Reproducibility of α, t data from Fig. 1. Three separate runs at 369°C are shown. This is typical of the reproducibility obtained.

395°C the curves are superimposable within reproducibility limits. This indicates that the in situ dehydration process in vacuum is not influencing the overall thermal decomposition—presumably the dehydration is rapid and essentially complete before the thermal decomposition process begins.

(b) Interrupting the decomposition at various times and exposing the sample to a saturated water vapor atmosphere for 20 min does not significantly alter the general features of the overall shape of the subsequent thermal decomposition plot. For interruption times falling during the decay period the curves were initially faster than the original curve but eventually reached the same, slow decay rate as the original curve prior to exposure. This initial fast rate is attributable to the water vapor interacting with the partially-decomposed solid to expose fresh (unreacted) surface which would decompose more rapidly. Faster initial rates were also observed for samples interrupted during the acceleratory period but were always deceleratory throughout; the water vapor presumably penetrating the reactant and breaking it up into smaller particles which rapidly react and then follow a contracting interface type of behaviour. Interruption during the induction period appears to lengthen this period slightly; presumably the water vapor removes some nucleation (surface?) sites and the thermal reaction requires a longer time for the nucleation process to become operative at other reaction sites.

(c) The solid decomposition products may catalyze the decomposition.

However, when a 1 : 1 molar ratio mixture of pristine powder and MgO, the final product, were decomposed, the same α, t curves were found as those for pristine material, within experimental error. Thus, the reaction is unaffected by the presence of MgO.

(d) To test whether certain gases catalyze or retard the thermal decomposition, samples were decomposed at 395°C in ~ 120 torr partial pressures of N_2 and O_2 gases respectively. The resulting plots do not differ from those from the samples decomposed in vacuo or each other over the extent of the sigmoidal curve (i.e. up to $\alpha \sim 0.50$) but for the N_2 curve the point of onset of the long slow rate at this α value becomes abrupt and well defined and the final rate is slower and markedly linear. No significant difference was observed between the O_2 pressure curve and the sample decomposed in vacuo. Presumably N_2 gas has a selective effect on the slow decomposition, possible suppressing sublimation as reported by Acheson and Jacobs [8].

(e) Examination of the morphology of dehydrating particles indicates that they do not physically disintegrate or decrepitate during the reaction in vacuum. The crystals remain intact but easily crumble into a fine powder if mechanically disturbed. Melting does not occur in vacuum. On completion of the thermal process the residue exhibits a smooth surface indicative of a sublimation process.

Kinetic analysis of α, t, *data*

The various stages of the decomposition were subjected to several kinetic analyses. (In analyzing the α, t data, the value of α_0, the fractional decomposition corresponding to the completion of the first, sharp decay period was chosen to be that corresponding to the onset of the slow rate, i.e. the α value corresponding to the time that the α vs. t data was not fitted by the kinetic curve used to fit the long, slow rate.)

The rate constant for the induction period, k_1, was determined from

$$1/\tau = k_1 \tag{3}$$

where τ is the time at which the induction period diverges from linearity.

The acceleratory period rate constant, k_2, was determined by fitting the data to the equation

$$\alpha^{1/2} = k_2 t + c_2 \tag{4}$$

Comparisons with the cubic equation [12], the Prout–Tompkins [15] (PT) equation and the Avrami–Erofeyev (A–E) equation [16] showed that while PT and A–E equations clearly did not describe the data, the cubic equation gave a reasonably good fit over some of the curves. The cubic equation was rejected eventually because its extent of fit did not cover the range of eqn. 2 uniformly over the temperatures studied.

Above 420°C an additional acceleratory period is observed following the

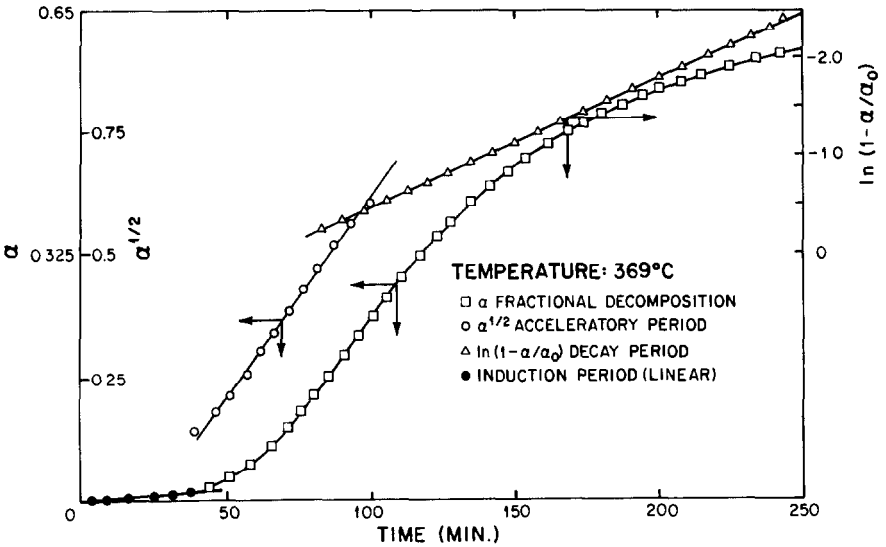

Fig. 4. Fractional decomposition, $\alpha = p(t)/p_f$, vs. time and kinetic analysis (α, induction period; $\alpha^{1/2}$, acceleratory period; $\ln(1-\alpha/\alpha_0)$, decay period, vs. time) for $Mg(ClO_4)_2$ powder decomposed isothermally at 369°C in vacuo. The estimation of α_0 is described in the text.

sharp decay. This period was also fitted to eqn. 2 over its entire range of $\alpha \sim 0.4$ to 0.95. The reaction terminated too rapidly for any quantitative fitting to be made of the decay period of the second reaction.

TABLE 1

Thermal decomposition rate constants for the induction, k_1, acceleratory (2 stages), k_2, decay, k_3, and slow rate, k_4, periods in $MgClO_4 \cdot 6H_2O$ powder [a]

Decomposition temperature (°C)	k_1 [b]	k_2 [b]		k_3 [b]	k_4 [c]
369	2.19	0.687		1.33	0.221
379	5.0	1.04		1.90	0.266
386	10.0				
395	24.0	1.85		2.93	0.473
400		2.73		4.81	0.654
405		3.16		6.77	0.987
410		4.89		10.10	2.32
417		15.1		23.90	7.41
420		17.0	0.0410		
423		23.0	0.0785		
426		31.8	0.0819		
429		39.9	0.0796		

[a] All k values in units of 10^{-2} min^{-1}.
[b] Maximum error ±5%.
[c] Maximum error ±4%.

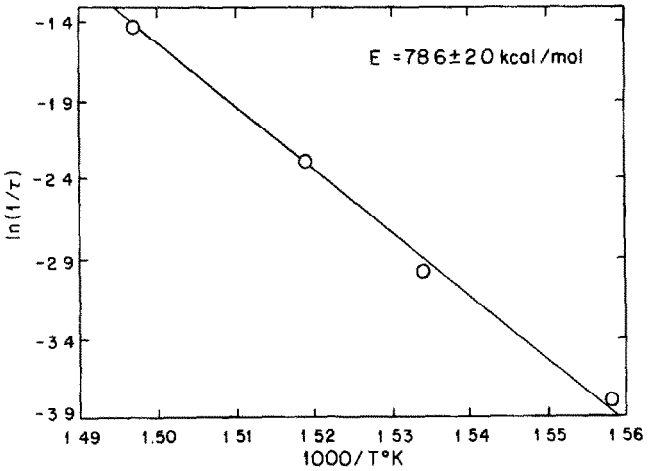

Fig. 5. Plot of ln(rate constant) vs. $1/T$ K for the induction period of the thermal decomposition of magnesium perchlorate powder.

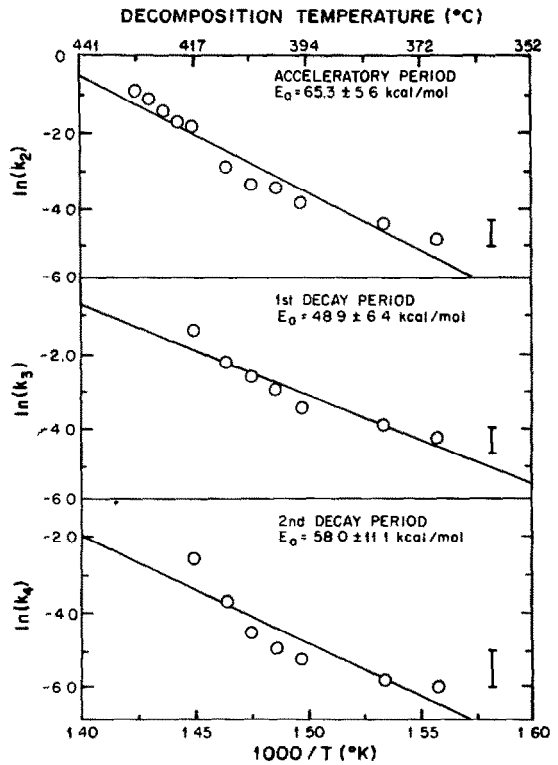

Fig. 6. Plot of ln(rate constant) vs. $1/T$ K for the acceleratory, short and long decay periods of the thermal decomposition of magnesium perchlorate powder.

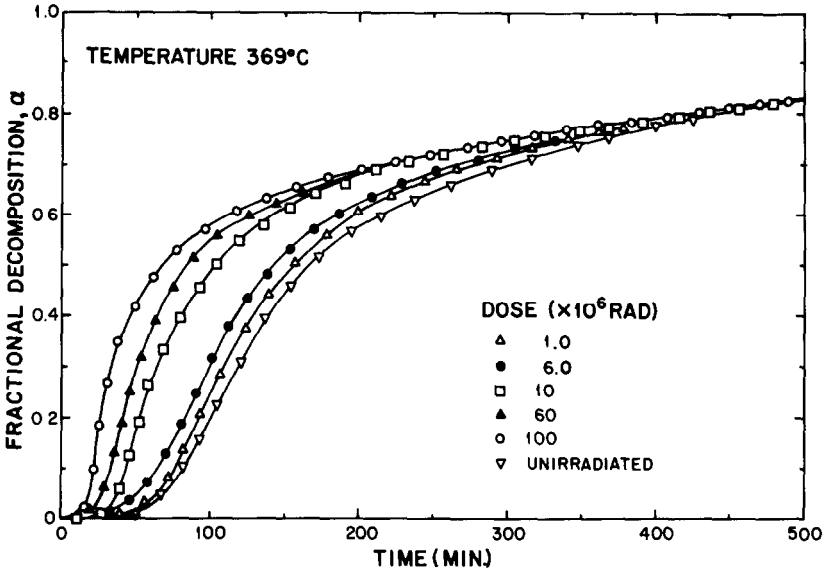

Fig. 7. Effect of gamma irradiation on the subsequent thermal decomposition of dehydrated magnesium perchlorate powder. The plot shows the fraction decomposition, α, vs. time for gas evolution from powder at 369°C.

The short, sharp decay stage and the subsequent long, linear component were fitted to the unimolecular decay law in the form

$$\ln(1 - \alpha/\alpha_0) = k_3 t + c_3 \tag{5}$$

for the short decay period, where α_0 is the value corresponding to the onset of the slow rate and, for the long, slow rate

$$\ln(1 - \alpha) = k_4 t + c_4 \tag{6}$$

was found to be best fit.

A typical fit of eqns. 1, 2 and 3 to the sigmoidal region of the α, t curve at 369°C is shown in Fig. 4. The rate constants k_{1-4} were determined from eqns. 3–6. These are shown in Table 1.

Figures 5 and 6 are plots of ln k_1 and ln $k_{2,3,4}$ vs. $1/T$ K, respectively. Activation energies of 78.6 ± 2.0; 65.3 ± 5.6; 48.9 ± 6.4 and 58.0 ± 11.1 kcal mol^{-1} resulted from these plots, respectively. The rate constant for the high temperature acceleratory period did not vary within experimental error over the 6°C temperature range.

In addition a series of experiments was carried out to examine the effects of exposing dehydrated material to ^{60}Co gamma rays prior to decomposition. The resulting α, t plots at 369°C for gamma doses ranging from 1.0×10^6 to 1.0×10^8 rad are shown in Fig. 7, with data from an unirradiated sample included for comparison. The samples were dehydrated prior to irradiation and were prepared by successive heating of pristine sieved

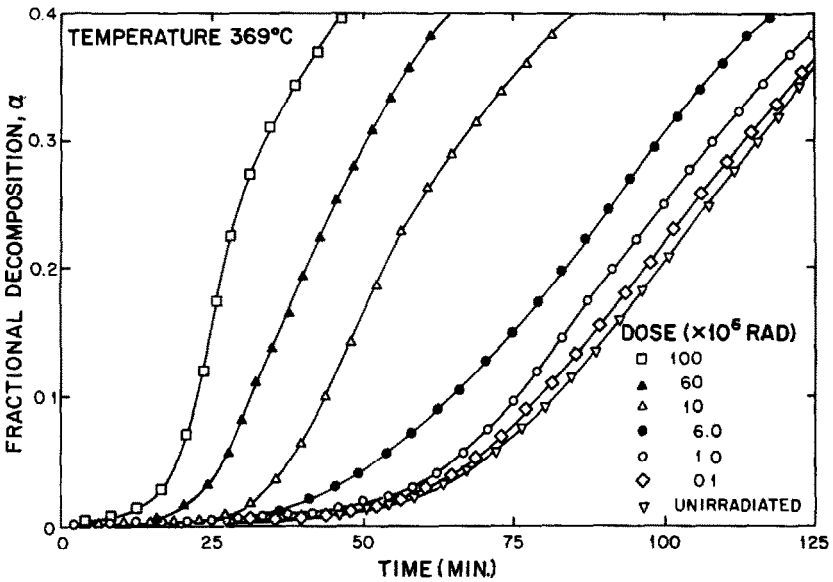

Fig. 8. Detail of Fig. 12. Effect of gamma radiation on the induction and acceleratory period of the isothermal decomposition of dehydrated magnesium perchlorate at 369°C.

materials in vacuo (below 0.5 mmHg) with P_2O_5 traps at 170°C for 1 h followed by 15 h at 230°C with fresh P_2O_5. The dehydrated material was encapsulated under dry nitrogen.

The principal effects of doses above 1.0×10^5 rad are to shorten the induction period and to increase the rate of the acceleratory period while

TABLE 2

Thermal decomposition rate constants for the induction, k_1, acceleratory, k_2, and short, k_3, and long, k_4, decay periods of irradiated $Mg(ClO_4)_2$. Decomposition temperature 369°C. (All k values in units of 10^{-2} min^{-1})

Dose ($\times 10^6$ rad)	k_1 [a]	k_2 [b]	k_3 [c]	k_4 [d]
Unirradiated	2.19	0.687	1.33	0.221
0.1	2.20	0.753	2.11	0.252
1.0	2.60	0.794	2.57	0.268
6.0	2.90	0.718	1.57	0.235
10.0	3.30	1.40	1.55	0.172
60.0	5.80	1.71	1.92	0.254
100.0	9.60	2.76	1.84	0.194

Maximum error:
[a] <1%;
[b] ±4.7%;
[c] ±1%;
[d] ±1%.

reducing its extent, i.e., the inflexion point is lowered with increasing dose. This is shown in detail in Fig. 8. The irradiated samples were cream in color with the intensity of the color increasing with dose. The color begins to fade once the ampoules are opened. The irradiated samples exhibit a chlorine-like odor.

The irradiated data were fitted to the same kinetic equations used for the unirradiated data and the resulting rate constants (k_1, k_2, k_3 and k_4), are shown in Table 2 as a function of gamma-ray dose. Although displaying an unusually large scatter, the decay rates, both slow and fast, are essentially unaffected by exposure to the irradiation. Presumably the reactant particles are sufficiently reduced in size after the acceleratory period to have reached a limiting value. The reduction of the inflexion point to lower α values with increasing dose reflects the more rapid nucleation and growth of product induced by the additional radiation-induced nuclei to reach the size limit. This effect increases monotonically with dose. A similar effect occurs over the induction period where the length of the period varies linearly with the $\log_{10}$ (dose).

Differential scanning calorimetry

The DSC trace of $Mg(ClO_4)_2 \cdot 6H_2O$ contains several peaks (Fig. 9). Three distinct endotherms are evident at 148, 248 and 344°C, and two exotherms 410 and 473°C respectively. Sequential interruption after each

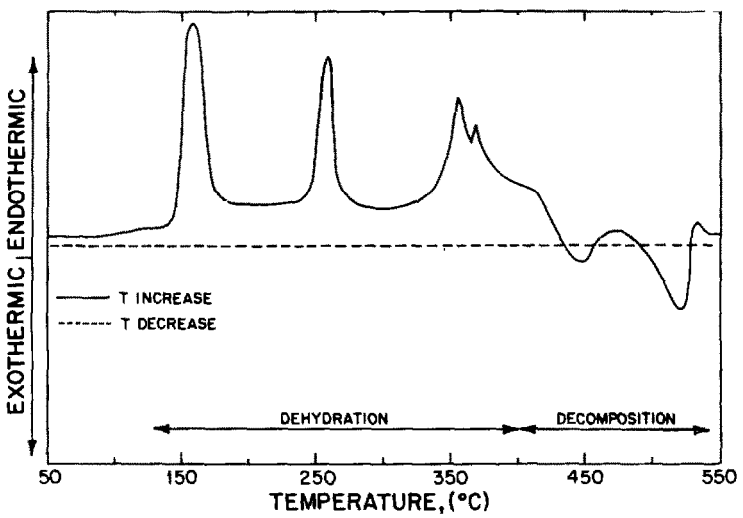

Fig. 9. Differential scanning calorimeter trace from 10.0 mg $Mg(ClO_4)_2 \cdot 6H_2O$ from 50 to 550°C. Scanning rate 10° min^{-1}. This curve illustrated the dehydration (below 400°C) and thermal decomposition of $Mg(ClO_4)_2$ (above 400°C).

TABLE 3

Heats of dehydration, fusion, decomposition and visual observation of events occurring during the decomposition of $Mg(ClO_4)_2 \cdot 6H_2O$ from DSC at atmospheric pressure

Temp. (°C)	ΔH (kcal mol^{-1})	Associated reaction	Visual observation
148–197	Endo 51.8 ± 0.13	[c] Dehydration + fusion $Mg(ClO_4)_2 \cdot 6H_2O(s) \rightarrow Mg(ClO_4)_2 \cdot 4H_2O(s)$	
148–155	Endo 11.6 ± 1.0	[a] Fusion $Mg(ClO_4)_2 \cdot 4H_2O(s) \rightarrow Mg(ClO_4)_2 \cdot 4H_2O(s)$	
180–190			Sample melts (colorless), melt begins to thicken and is solid by 250°C
200–250		$Mg(ClO_4)_2 \cdot 4H_2O(l) \rightarrow Mg(ClO_4)_2 \cdot 3H_2O(s)$	
248–278	Endo 24.2 ± 5.0	[c] Dehydration + fusion $Mg(ClO_4)_2 \cdot 3H_2O(s) \rightarrow Mg(ClO_4)_2 \cdot 2H_2O(l)$	Sample melts again by 265°C
246.6	Endo 7.5 ± 0.2	[b] Fusion	
253.6	Endo 4.8 ± 2.1	[c] $Mg(ClO_4)_2 \cdot 2H_2O(s) \rightarrow Mg(ClO_4)_2 \cdot 2H_2O(l)$	
275			Slight yellowing of melt boiling (bubbling) of melt, yellow color changes to white
320–350			
344–395	Endo 27.3 ± 0.9	[c] Dehydration $Mg(ClO_4)_2 \cdot 2H_2O(l) \rightarrow Mg(ClO_4)_2(s)$	Solid white residue
385			
410–478	Exo 36.9 ± 8.0	Decomposition in 2 stages	White residue remains
473–533	Exo 39.8 ± 2.6	$Mg(ClO_4)_2(s) \rightarrow MgO(s) + Cl_2(g) + 7/2O_2(g)$	

[a] Reversible below 248°C.

[b] Reversible below 400°C.

[c] TGA results confirm loss of $2H_2O$ from 150 to 250°C.

peak followed by cooling produces several interesting effects:

(a) interrupting after the first endotherm and cooling results in a reversible reaction indicative of a melting process;

(b) interruption after the second endotherm and cooling results in a reversible smaller endotherm with the removal of the initial larger endotherm. Again this would seem to indicate a melting process associated with the initial second endotherm;

(c) interruption after the third endotherm and cooling results in the removal of all three endotherms;

(d) interruption after the first exotherm and cooling to ~ 400°C does not regenerate the first exotherm. However cooling to room temperature and then recycling will produce both exotherms on reheating. Similar results were reported previously [13,14] for the disappearing and reappearing of oxygen peaks by cycling above and below 165°C. Presumably this result points to the thermal decomposition process involving the presence of an unstable intermediate;

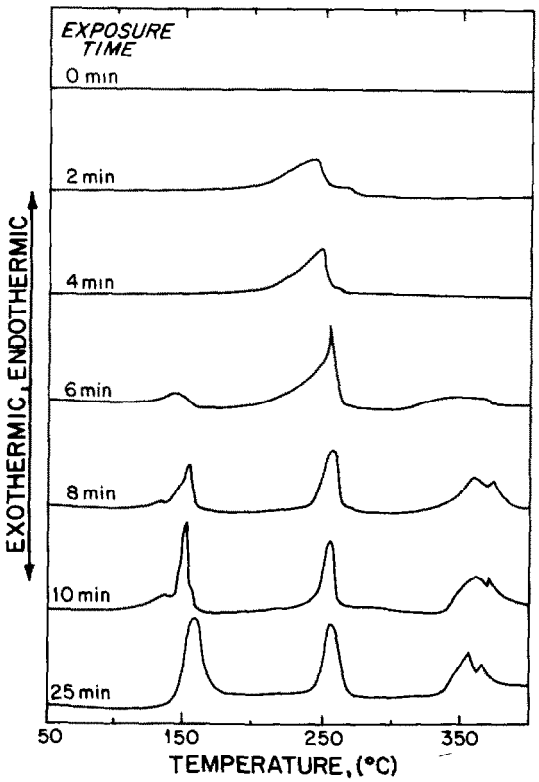

Fig. 10. Rehydration of dehydrated magnesium perchlorate powder. The effects of exposure to saturated water vapor atmospheres at 25°C for various times indicated on the subsequent DSC trace of dehydrated magnesium perchlorate powder between 50 and 400°C. Scanning rate 10° min^{-1}.

(e) after completion of the reaction at 550°C on cooling no peaks are detectable.

Visual observations of the reaction in the DSC support the formation of molten material corresponding to the temperatures at which reversible peaks are observed (Table 3). Heats of dehydration, fusion and decomposition were calculated from the areas under the curves and are tabulated in Table 3.

Rehydration of dehydrated material occurs sequentially. The effects of exposing dehydrated samples to saturated water vapor at 25°C for various times on the subsequent DSC trace is shown in Fig. 10. The second endotherm grows in initially followed by traces of the first and the third. These latter two grow in at a faster rate as the exposure time increases and the sample is completely rehydrated after 25 min exposure at 25°C.

Thermogravimetric analysis

The results found in the DSC measurements are supported by the thermogravimetric data. Hydrated magnesium perchlorate exhibits a fractional weight loss which begins at ~ 150°C coincident with the onset of the first DSC endotherm. Marked overlapping occurs in the subsequent dehydration curves but three discrete deceleratory weight loss increments can be discerned corresponding to ~ $2H_2O$ each. Comparison of this data to the

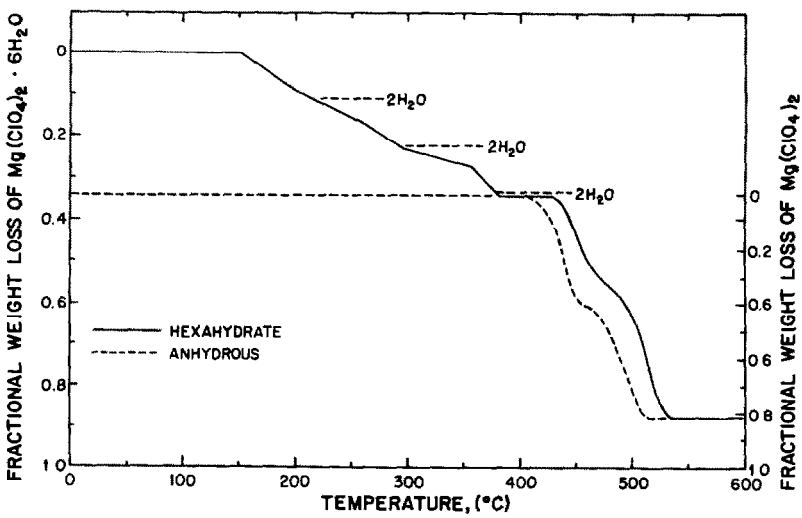

Fig. 11. Fractional weight loss during the thermal gravimetric analysis of 9.12 mg of $Mg(ClO_4)_2 \cdot 6H_2O$ and 9.88 mg of dehydrated $Mg(ClO_4)_2$ from room temperature to 600°C. The sample was swept with dry nitrogen gas during decomposition. Scanning rate 10°C min^{-1}.

theoretical values in shown in Fig. 11. Clearly all the water is removed by 395°C prior to the onset of the thermal decomposition exotherms.

The thermal process occurs in two stages both present in previously dehydrated material and in material dehydrated in situ. The previously dehydrated material decomposes faster due to the finer particle size of the material. However, the amount of material thermally decomposed in each stage in both samples is approximately half of the total available for decomposition.

X-ray diffraction patterns

Specimens were encapsulated and measured after decomposing to temperatures corresponding to each DSC peak indicative of the removal of each set of $2H_2O$ molecules. The resulting powder diffraction patterns are complex and differ from each other. Detailed analysis of these spectra were not possible as crystallographic data for the partially hydrated material is unavailable.

DISCUSSION

Dehydration

The thermal dehydration process in $Mg(ClO_4)_2 \cdot 6H_2O$ is complex. The overall process occurs in several stages and is best understood by considering the DSC scans, TGA data and visual observations together. In air the samples dehydrate in three distinct temperature regions characterized by the three large endotherms at (150–190), (240–280) and (325–400)°C, respectively. Each of these endotherms represent a stage of the decomposition and will be considered separately.

Between 150 and 190°C, 2 mol of water are evolved. This process begins at 150°C and is complete at 190°C. However the formation of $MgClO_4 \cdot 4H_2O$ is also accompanied by melting, the sample being completely molten at 190°C. This solid/liquid phase transformation is reversible with $\Delta H_{fusion} = 11.6 \pm 1.0$ kcal mol^{-1}. The initial large endotherm contains both the ΔH_{fusion} and $\Delta H_{dehydration}$: the latter was found by subtraction and is 4.0 ± 1.0 kcal mol^{-1}. X-ray data of molten material quenched to room temperature and analyzed indicates the presence of a new phase.

From 190°C to the onset of the next isotherm at 240°C no endo- or exothermic reaction is observed but the sample continues to lose weight; indeed almost another 1 mol of H_2O has been removed when the temperature of the onset of the second endotherm is reached, but no detectable amount of heat is absorbed or generated during this process. However visual observations indicate that the molten material thickens either by a slow

resolidification process or by formation of a eutectic with a solid precipitate. The solid mass of material continues to lose up to another mol of H_2O between 240°C and 280°C. This process is again accompanied by re-melting of the entire sample: The stoichiometry of this material is $MgClO_4 \cdot 2H_2O$. This fusion process is reversible with a $\Delta H_{fusion} = 12.25 + 2.1$ kcal mol^{-1}. The $\Delta H_{dehydration}$ of the second large endotherm is found by subtraction to be 10.0 ± 5.0 kcal mol^{-1}. The nature of the intermediate is unclear at this stage. It may be $MgClO_4 \cdot 3H_2O$ but no clear evidence (DSC or TGA) exists for its stability. Most likely it is a eutectic solid solution involving $Mg(ClO_4)_2 \cdot 4H_2O$ (melt) and $Mg(ClO_4)_2 \cdot 2H_2O$ (solid). Occasionally two reversible peaks are observed close together during the fusion process (see Table 3); one possibility is that the fusion process is preceded by a structural transformation.

Weight loss continues slowly from 280 to 325°C, again associated with a thickening of the melt, presumably with the precipitated (anhydrous) material. The removal of the final $2H_2O$ is accomplished by 400°C and a solid residue remains. This solid residue is crystallographically distinct from the two other hydrates. The $\Delta H_{dehydration}$ for the final process is 27.3 ± 0.9 kcal mol^{-1}.

The effect of decreasing the partial pressure above the material to below 0.5 torr before dehydration is to produce a solid residue which shows no evidence of premelting. Indeed the α, t curves of thermally-decomposed hydrated and dehydrated powder at 369°C are superimposable indicating no pronounced change in the sample morphology by dehydrating in vacuo. Presumably the dehydration simply occurs more effectively in vacuo.

The rehydration at atmospheric pressure supports the concept of the dehydration occurring in stages. After a short exposure (2 min) to saturated water vapor, sufficient $Mg(ClO_4) \cdot 2H_2O$ is formed on the surface to produce a fusion type endotherm between 240 and 280°C but this water is lost prior to the formation of the final endotherm which is not observed at this low concentration. As the H_2O concentration is built up the $Mg(ClO_4)_2 \cdot 2H_2O$ peak is more pronounced and the $6H_2O \rightarrow 4H_2O$ peak and $2H_2O \rightarrow OH_2O$ peaks become detectable and eventually reach equilibrium.

Thermal decomposition

The thermal decomposition in vacuo above 369°C involves two processes. Below 417°C, the sigmoidal α, t plots comprise a linear induction period, during which the reaction nucleates at energetically favorable sites. These nuclei would be relatively small initially and grow two-dimensionally to a larger size over the acceleratory period. The growth occurs over the surface and along surface boundaries of the powder until eventually a uniform interface is formed and the reaction becomes deceleratory. This occurs relatively early in the extent of the reaction ($\alpha \sim 0.25$). The unimolecular law

then adequately describes the reaction until completion. The short decay period terminates close to $\alpha \sim 0.5$ and is followed by an extremely long slow reaction which has been associated with decomposition of the intermediate and slight surface sublimation. This very slow reaction accelerates rapidly as the temperature increases; above 417°C the decay stage becomes sigmoidal in shape to include an additional acceleratory period which is fitted by another growth type equation. Presumably the formation of the product of the reaction at $\alpha \sim 0.5$ involves an intermediate which can be decomposed rapidly above 417°C. The activation energies for the process are: induction period, 78.6 ± 2.0 kcal mol^{-1}, acceleratory period, 65.3 ± 5.6 kcal mol^{-1}, and the decay stages, 48.9 ± 6.4 and 58.0 ± 11.1 kcal mol^{-1}, respectively.

The mechanism of the decomposition must involve a two-stage process with the formation of a stable intermediate at an α value of 0.5. A viable compound for the intermediate is that proposed earlier by Borisova et al. [14]

$$2Mg(ClO_4)_2 \rightarrow [MgO \cdot Mg(ClO_4)] + Cl_2 + 3.5O_2 \quad (7)$$

$$[MgO(MgClO_4)] \rightarrow 2MgO + Cl_2 + 3.5O_2 \text{ (decomposition)} \quad (8)$$

$$\rightarrow MgO + Mg(ClO_4)_2 \text{ (dissociation and reformation)} \quad (9)$$

X-ray diffraction evidence supports the formation of an intermediate of the type illustrated in eqn. 7; the diffraction pattern at various stages of the decomposition is made up of only MgO and $Mg(ClO_4)_2$ components and no MgCl was detected.

The shortening of the induction period by the irradiation and the increasing in the acceleratory rate can be attributed to the formation of additional nucleation sites. Also, for a given gamma dose, the radiation produced nuclei are formed in concentrations in the bulk greater than those normally present. The relative increase in concentration of nuclei in the irradiated samples can be shown quantitatively by considering the relationship between the induction period length, I, with irradiation dose, ϕ. It has been established (Fig. 12) that the thermal induction period of the above-mentioned materials is experimentally related to the radiation dose, ϕ, by the equation

$$I = c_1 - c_2 \log \phi \quad (10)$$

A specific combination of thermal and radiation-induced processes has been shown to produce this relationship [16]. The resulting equation is of the form

$$I = 1/g \ln[N_0/N_c + j/N_c\phi] \quad (11)$$

where g and j are constants and N_0 and N_c are the initial and critical size of the nucleus at time $t = 0$ and $t = I$ respectively. The fit of eqn. (11) to the I and ϕ data obtained at 369°C is shown in Fig. 12. The equation was calculated using the linear high-dose data and the induction period data of unirradiated material. A basic tenet of eqn. 11 is that $N_c/N_0 \gg 1$. From the fit shown in Fig. 12 a value of 658 for N_c/N_0 was obtained. The results for

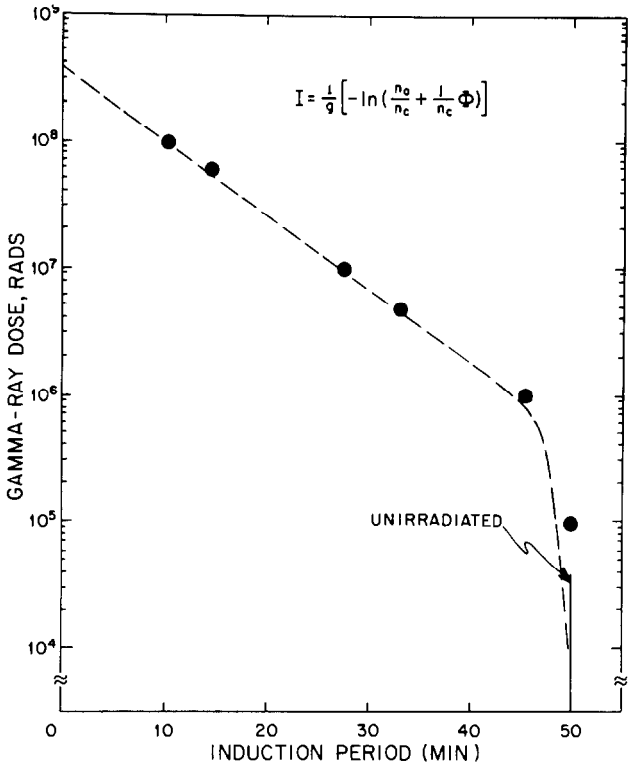

Fig. 12. Induction period vs. total gamma-ray dose data for $Mg(ClO_4)_2$ powder decomposed at 369°C. The dashed line was computed from eqn. 11 in text by using the linear high dose data and the length of the induction period for the unirradiated material.

TABLE 4

Material	Decomp. temp. (°C)	Induction period for unirradiated material (min)	Type of radiation	Ratio N_c/N_0
KMnO4	210	47	^{60}Co rays	2.0×10^4
	224	65	Reactor	7.6×10^4
	224	65	^{60}Co rays	1.2×10^3
$NaMnO_4$	140	101		1.15×10^2
$RbMnO_4$	230	103		3.2×10^2
$CsMnO_4$	240	167		1.3×10^4
BaN_6	110	180		4.9×10^8
NH_4ClO_4	227	63		6.75×10^4
	238	39		1.4×10^4
	135	19400		1.22×10^4
$LiAlH_4$	130	38		6.3×10^4
α-AlH_3	110.6	135		2.1×10^6
$Mg(ClO_4)_2$	369	50		6.58×10^2

all previously determined materials, including those for $Mg(ClO_4)_2$ are tabulated in Table 4. Clearly, as predicted, N_c/N_0 is consistently greater than 1.

SUMMARY

The molar heats of dehydration, fusion and decomposition of $Mg(ClO_4)_2 \cdot 6H_2O$ have been evaluated for the dehydration process and the thermal decomposition over the temperature range 50–500°C. Dehydration occurs in three distinct temperature regimes, each associated with the removal of $2H_2O$. The thermal decomposition of $Mg(ClO_4)_2$ occurs in two stages with the formation of an intermediate, $MgO[Mg(ClO_4)]$. The decomposition is accelerated by prior exposure to gamma rays and the reduction in the length of the induction period with increasing gamma dose can be explained in terms of a previously derived theory.

ACKNOWLEDGMENT

This research was supported by a grant from the U.S. Naval Air Systems Command, Contract No. N00019-84-M-0318.

REFERENCES

1 W.E. Brown, D. Dollimore and A.K. Galwey, in C.H. Bamford and C.F.H. Tipper, (Eds.), Comprehensive Chemical Kinetics, Elsevier Scientific Publishing Co., New York, 1980, Vol. 22, 35.
2 P.J. Herley and P.W. Levy, J. Chem. Phys., 49 (1968) 1493.
3 P.W. Levy and P.J. Herley, J. Phys. Chem., 75 (1971) 191.
4 G.F. Smith and H.H. Willard, J. Am. Chem. Soc., 44 (1922) 2255.
5 G.F. Smith, O.W. Rees and V.R. Hardy, J. Am. Chem. Soc., 54 (1932) 3513.
6 L.E. Copeland and R.H. Bragg, J. Phys. Chem., 58 (1954) 1075.
7 G.G. Marvin and L.B. Woolaver, Ind. Eng. Chem., Anal. Ed., 17 (1945) 474.
8 R.J. Acheson and P.W.M. Jacobs, J. Phys. Chem., 74 (1970) 281.
9 S. Gordon and C. Campbell, Anal. Chem., 27 (1955) 1102.
10 A.A. Zinov'ev and L.J. Cludinova, Zh. Neorg. Khim., 1 (1956) 1722.
11 F. Solymosi, Acta Chem. Acad. Sci. Hung., 57 (1968) 35.
12 P.W.M. Jacobs and F.C. Tompkins in W.E. Garner (Ed.), Chemistry of the Solid State, Butterworths, London, 1955, Chap. 7.
13 L.G. Bereykina, S.L. Borisova and N.S. Tamm, J. Chromatogr., 69 (1972) 25.
14 S.I. Borisova, L.G. Bereykina, N.S. Tamm and A.V. Novosclova, Kinetika i Katal., 16 (1975) 68.
15 E.G. Prout and F.C. Tompkins, Trans. Faraday Soc., 42 (1946) 468.
16 M. Avrami, J. Chem. Phys., 9 (1941) 177; B.V. Erofeyev, C.R. Acad. Sci. USSR., 52 (1946) 51.